

## The Phase Equilibria of Richterite and Ferrichterite

ROBERT W. CHARLES

University of California, Los Alamos Scientific Laboratory,  
CNC-11, M/S 514, Los Alamos, New Mexico 87544

### Abstract

The phase relations of the amphiboles richterite and ferrichterite have been defined using standard hydrothermal and oxygen buffering techniques. Richterite is stable to  $1030^\circ \pm 10^\circ\text{C}$  at 1 kbar  $P_{\text{total}}$ . Above 150 bars richterite decomposes to forsterite + diopside + enstatite + melt + vapor. Under conditions between  $930^\circ\text{C}$  at 50 bars and  $970^\circ\text{C}$  at 150 bars the decomposition assemblage is roedderite + forsterite + diopside + melt + vapor. Below  $930^\circ\text{C}$  and 50 bars, richterite reacts to roedderite + 1:2:6 Na-Mg silicate + forsterite + diopside + vapor. Ferrichterite on the iron-wüstite (IW) buffer is stable to  $715^\circ \pm 5^\circ\text{C}$  at 1 kbar  $P_{\text{total}}$ , decomposing to hedenbergitic pyroxene + fayalite + melt + vapor at higher  $T$ . Below 600 bars ferrichterite decomposes to 1:2:6 Na-Fe silicate + hedenbergitic pyroxene + fayalite + melt + vapor. Ferrichterite on the quartz-fayalite-magnetite (QFM) buffer is stable to only  $525^\circ \pm 20^\circ\text{C}$  at 1 kbar, reacting to form acmite<sub>67</sub>hedenbergite<sub>33</sub> + fayalite + magnetite + quartz + vapor at higher  $T$ . Above  $820^\circ \pm 10^\circ\text{C}$  at 1 kbar, this assemblage undergoes partial melting to form hedenbergitic pyroxene + fayalite + magnetite + melt + vapor. Above IW the ferrichterite bulk composition yields amphibole + acmitic pyroxene, indicating that completely ferrous ferrichterite is stable only at very low  $f_{\text{O}_2}$ .

### Introduction

The phase equilibria of magnesium- and iron-bearing amphibole end members have been examined extensively for three amphibole series: tremolite (Boyd, 1959)-ferrotremolite (Ernst, 1966); pargasite (Boyd, 1959)-ferropargasite (Gilbert, 1966); magnesioriebeckite (Ernst, 1960)-riebeckite (Ernst, 1962). The phase relations of these series along with work on other amphibole end members have been summarized by Ernst (1968). The richterite series presented here adds information concerning the effect of the  $\text{Na} \rightleftharpoons \text{Ca}$  and  $\text{Mg} \rightleftharpoons \text{Fe}$  substitution upon thermal stabilities and physical properties of amphiboles.

Richterites are monoclinic amphiboles composed of double chains of silicon tetrahedra. The cation sites linking these chains contain Na in the 8-fold  $A$  site, Na and Ca in the 8-fold  $M(4)$  sites, and Mg and Fe in the remaining 6-fold  $M$  sites.

Richterites, though uncommon, are found in rather varied low-pressure and high-temperature environments. Earlier investigations and some natural occurrences were given in a previous article (Charles, 1974).

### Experimental

Oxide mixes of appropriate bulk compositions were prepared for both richterite and ferrichterite.

Na was added as  $\text{Na}_2\text{Si}_2\text{O}_5$ . Mixes containing both hematite and native iron were prepared for ferrichterite. These mixes were used interchangeably to check equilibrium on the oxygen buffer used.

The oxide mixes were subjected to temperature and pressure in standard cold-seal vessels, in an internally heated vessel, or in 1-atm quench furnaces, depending upon the conditions desired. Oxygen fugacities were buffered with standard solid buffering techniques (Eugster, 1957), direct hydrogen diffusion (Shaw, 1967), and graphite-methane buffering (Eugster and Skippen, 1967).

Unit-cell dimensions were determined using  $\text{BaF}_2$ , Baker lot No. 308 ( $a = 6.1971 \pm 0.0020 \text{ \AA}$ ), as an internal standard for the powder diffraction patterns. The cell parameters were calculated using the program of Evans, Appleman, and Handwerker (1963).

### Results<sup>1</sup>

#### Richterite

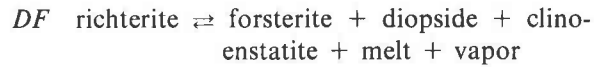
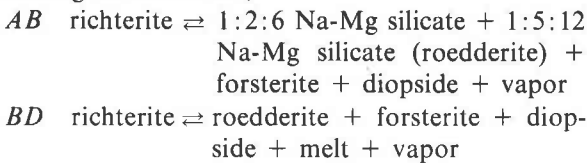
Figure 1 presents the stability relations of Mg-richterite for the  $P$ - $T$  region  $800^\circ$  to  $1150^\circ\text{C}$  and 0 to

<sup>1</sup> Table 1 lists the abbreviations used in this paper, and Table 2 lists the bracketing experiments from which the stability relations were determined.

TABLE 1. Key to Abbreviations

A	Amphibole	Ro	Roederite
Ac	Acmite	V	Vapor
Cpx	Clinopyroxene	1:2:6	1:2:6 Na-(Mg,Fe) silicate
Di	Diopside	( )	Products in parentheses: ~5% content
En	Enstatite		
Fa	Fayalite		
Fo	Forsterite	<u>Buffers:</u>	
H	Hematite	C-CH <sub>4</sub>	Graphite-methane
Hd	Hedenbergite	HM	Hematite-magnetite
L	Liquid	IW	Iron-wüstite
M	Melt	NNO	Nickel-nickel oxide
Mix	Reduced mix (Fe <sup>o</sup> )	QFM	Quartz-fayalite-magnetite
Mt	Magnetite	WM	Wüstite-magnetite
Q	Quartz		

1000 bars  $P_{\text{total}} = P_{\text{H}_2\text{O}}$ . The univariant equilibria involving richterite are,



Curves *BC* and *DE* are complex melting relations involving the disappearance of 1:2:6 Na-Mg silicate and roederite, respectively. *BC* and *DE* involve more than simple melting of these compounds since the work of Schairer and Yoder (1970) shows that, at 1 atm, 1:2:6 Na-Mg silicate melts at 1040°C and roederite melts at 1200°C. Richterite bulk composition consists of five components, and seven univariant curves must emanate from each invariant point. Those shown were found using a mix of richterite bulk composition.

Within its stability field Mg-rich richterite crystallized essentially 100 percent pure. Experiments at 800°C and 2 kbar of 2-3 days duration yielded 98-100 percent amphibole. This amphibole had the following properties:  $a = 9.902(1) \text{ \AA}$ ,  $b = 17.980(4) \text{ \AA}$ ,  $c = 5.269(1) \text{ \AA}$ ,  $V = 909.4(3) \text{ \AA}^3$ ,  $\beta = 104^\circ 13'(1)$ ,  $\alpha = 1.604(5)$ ,  $\gamma = 1.622(3)$ . All experiments in the field forsterite + diopside + enstatite + melt + vapor at 1 kbar produced 10-20 percent quench amphibole. This amphibole consisted of fine isotropic needles compared with the large ( $20 \times 40 \mu\text{m}$ ) pyroxenes and irregularly shaped forsterites. Experiments at 200 bars and beyond the amphibole field produced almost no quench amphibole. The term "clinostenatite" refers to a clinopyroxene near enstatite composition, but some solid solution with the diopside molecule and vice versa is certainly probable (Boyd and Schairer, 1964). The stable form of enstatite under these conditions is orthorhombic and will be referred to henceforth simply as "enstatite." Its 221 and 310 reflections appeared in the powder X-ray diffractometer patterns from the products of experiments of more than 2 days duration. Shorter experiments yielded forsterite + diopside + melt + vapor with possible small amounts of enstatite, which are difficult to distinguish optically from diopside.

Roederite ( $a = 10.147(1) \text{ \AA}$ ,  $c = 14.240(3) \text{ \AA}$ ) and 1:2:6 Na-Mg silicate were identified using the diffractometer patterns of Schairer and Yoder (1970). Neither may be stoichiometric, because addition of some Ca is possible without changing the unit-cell parameters (Olsen, 1967).

Forbes (1971) indicated that richterite is about 80°C less stable at 200 bars and approximately 20°C less stable at 1 kbar than the results presented here. Experiments using forsterite + diopside + enstatite + melt + vapor as starting materials and held for 68

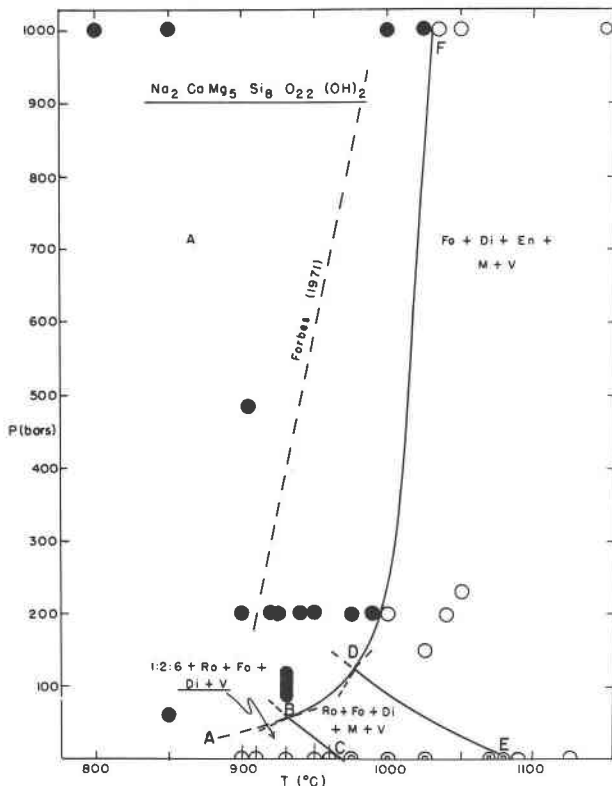


FIG. 1. Experimentally determined stability relations for Mg-rich richterite bulk composition. Symbol size approximates the errors in measuring  $P$  and  $T$ . Superimposed is Forbes' (1971) stability limit for Mg-rich richterite. ●, amphibole; ○, forsterite + diopside + enstatite + melt + vapor; ⊙, 1:2:6 Na-Mg silicate + roederite + forsterite + diopside + vapor; ○, roederite + forsterite + diopside + melt + vapor.

hours at 940°C and 200 bars produced >95 percent amphibole even though this is well beyond Forbes' stability limit. Experiments near the stability curve were duplicated two or three times using mix, decomposition products, or amphibole (see Table 2). In addition, this work has yielded the low-pressure field of 1:2:6 Na-Mg silicate + roedderite + forsterite + diopside + vapor.

TABLE 2. Bracketing Experiments for Bulk Compositions of Richterite and Ferrichterite

P (±15 bars)	T (±5°C)	Duration (hours)	Reactants	Products
<b>Na<sub>2</sub>CaMg<sub>5</sub>Si<sub>8</sub>O<sub>22</sub>(OH)<sub>2</sub></b>				
1000	1050	18	A	Fo+Di+En+Mt+ (A)
"	"	1035	"	"
"	"	"	1:2:6+Fo+Ro+Di	"
"	1025	"	A	A
"	"	7	Ro+Fo+Di+M	"
"	1000	18	"	"
200	1040	71	"	Fo+Di+En+M
"	1000	23-1/2	A	"
"	"	"	Fo+Di+En+M	"
"	990	27	1:2:6+Fo+Ro+Di	A
"	"	"	A	"
"	975	24	1:2:6+Fo+Ro+Di	"
1	1090	5	Fo+Di+En+M	Fo+Di+En+M
"	1080	4	Mix	Ro+Fo+Di+M
"	975	17-1/2	"	"
"	960	23	Ro+Fo+Di+M	1:2:6+Fo+Ro+Di
"	950	16	Mix	"
<b>Na<sub>2</sub>CaFe<sub>3</sub>Si<sub>8</sub>O<sub>22</sub>(OH)<sub>2</sub> (IW buffer)</b>				
5000	750	48	Cpx+Fa+M	Cpx+Fa+Mt+(A)
"	725	83	"	"
"	700	72	A	A
2000	750	47	"	Cpx+Fa+M
"	735	54	Cpx+Fa+M	"
"	725	63	"	A
1000	"	137	A	Cpx+Fa+Mt+(A)
"	"	48	Cpx+Fa+M	"
"	710	52	"	A
"	700	46	Cpx+Fa+M	"
750	725	41	"	Cpx+Fa+M
"	700	72	"	A
500	750	51	"	Cpx+Fa+M
"	720	52	"	1:2:6+Cpx+Fa+M
"	700	69	"	A
"	685	51	A	"
"	675	67	Cpx+Fa+M	A+(Cpx+Fa+M)
<b>Na<sub>2</sub>CaFe<sub>3</sub>Si<sub>8</sub>O<sub>22</sub>(OH)<sub>2</sub> (QFM buffer)</b>				
7000	850	28	Mix	Cpx+Fa+Mt+M
"	600	350	"	Ac <sub>67</sub> Hd <sub>33</sub> +Fa+Q+Mt
"	550	336	Ac <sub>67</sub> Hd <sub>33</sub> +Fa+Q+Mt	"
"	525	493	Mix	A+Cpx
5000	825	48	Ac <sub>67</sub> Hd <sub>33</sub> +Fa+Q+Mt	Cpx+Fa+Mt+M
"	800	72-1/2	"	Ac <sub>67</sub> Hd <sub>33</sub> +Fa+Q+Mt
"	550	310	"	"
"	525	336	"	A+Cpx
4000	700	162	"	Ac <sub>67</sub> Hd <sub>33</sub> +Fa+Q+Mt
"	525	356	"	A+Cpx
1000	835	52	"	Cpx+Fa+Mt+M
"	820	72	Cpx+Fa+Mt+M	"
"	800	117	Ac <sub>67</sub> Hd <sub>33</sub> +Fa+Q+Mt	Ac <sub>67</sub> Hd <sub>33</sub> +Fa+Q+Mt
"	"	65-1/2	Mix	"
"	550	504	Ac <sub>67</sub> Hd <sub>33</sub> +Fa+Q+Mt	"
"	525	"	"	A+Cpx
"	500	675	A+Cpx	"
"	450	2154	Ac <sub>67</sub> Hd <sub>33</sub> +Fa+Q+Mt	"
<b>Na<sub>2</sub>CaFe<sub>3</sub>Si<sub>8</sub>O<sub>22</sub>(OH)<sub>2</sub> (P<sub>total</sub> = 1 kbar)</b>				
Buffer				
HM	700	120	Oxidized Mix	Ac <sub>67</sub> Hd <sub>33</sub> +Fa+Mt+Q
"	"	"	Mix	"
"	"	"	Ac <sub>67</sub> Hd <sub>33</sub> +Fa+Q+Mt	"
NNO	850	96	"	Cpx+Mt+M
"	600	336	"	Ac <sub>67</sub> Hd <sub>33</sub> +Fa+Q+Mt
C-CH <sub>4</sub>	775	92	Cpx+Fa+M	Cpx+Fa+M
"	750	552	"	Ac <sub>67</sub> Hd <sub>33</sub> +Fa+Q
"	625	192	"	"
"	600	240	A+Cpx	A+Cpx
WM	775	48	Cpx+Fa+M	Cpx+Fa+Mt+(A)
"	750	"	"	A+(Cpx+Fa+M)

Abbreviations as in Table 1.

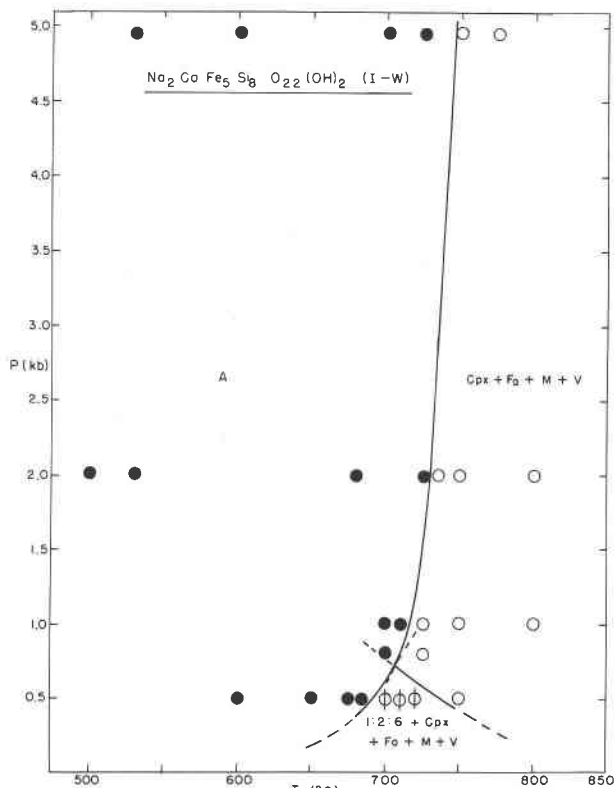


FIG. 2. Experimentally determined stability relations for ferrorichterite bulk composition with oxygen fugacities defined by the IW buffer.

Ferrichterite

The phase relations of the ferrous end member, ferrichterite, are presented in Figures 2, 3, and 4 and in Table 2. Figure 2 displays the relations of

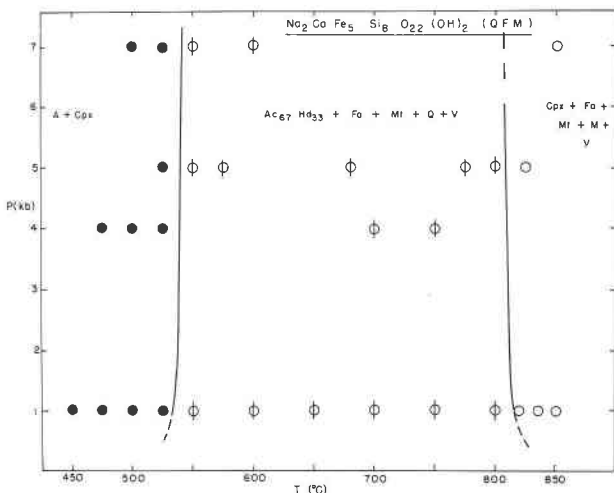


FIG. 3. Experimentally determined stability relations for ferrorichterite bulk composition with oxygen fugacities defined by the QFM buffer.

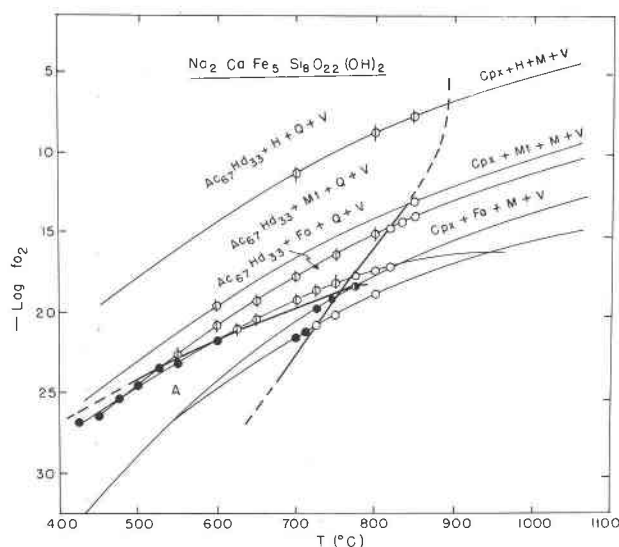


FIG. 4. Isobaric ( $P_{\text{total}} = 1$  kbar)  $\log f_{\text{O}_2}$ - $T$  diagram for ferrorichterite bulk composition. Field boundaries are dashed where inferred. In this diagram amphibole gradationally changes to amphibole + clinopyroxene as  $f_{\text{O}_2}$  increases until the stability limit of the remaining amphibole is reached. The buffer curves with decreasing oxygen fugacity are: hematite-magnetite, nickelbunsenite, quartz-fayalite-magnetite, graphite-methane, wüstite-magnetite, iron-wüstite, and iron-magnetite. Abbreviations as in Table 1.

ferrichterite in  $P$ - $T$  space at oxygen fugacities defined by the iron-wüstite (IW) buffer. At pressures greater than 700 bars, ferrichterite decomposes to hedenbergitic pyroxene + fayalite + melt + vapor. Reversals were obtained at 1, 2, and 5 kbar. Some metastable amphibole was observed in the decomposition region at 5 kbar but not at lower pressures. Reversal experiments contained amphibole crystallized for 20–30 days at 7–10 kbar and decomposition products grown at 800°C and 2 kbar for 2 days. Complete transformation of one assemblage to the other at >700°C was accomplished in experiments of only 3 days or less.

Below 700 bars ferrichterite reacts to form hedenbergitic pyroxene + 1:2:6 Na-Fe silicate + fayalite + melt + vapor. The 1:2:6 Na-Fe silicate decomposes to fayalite + melt at higher temperatures. The fayalite has a  $d_{130}$  of  $2.83 \pm 0.003$  Å and is believed to be pure  $\text{Fe}_2\text{SiO}_4$ , judging from the determinative curves of Fisher and Medaris (1969), since even a slight amount of Ca present in the olivine phase (fayalite-kirschsteinite) would strongly increase the  $d_{130}$  (Sahama and Hytönen, 1958).

The hedenbergitic pyroxene has the following cell parameters:  $a = 9.809(4)$  Å,  $b = 8.999(7)$  Å,  $c = 5.288(18)$  Å,  $\beta = 105^\circ 15'(7)$ ,  $V = 465.7(1.3)$  Å<sup>3</sup>.

Because of poor resolution of pyroxene peaks and interference with fayalite, only six reflections were used for refinement: 110, 220,  $\bar{2}21$ , 310, 311, and  $\bar{1}31$ . Refinements using these peaks generally yielded values of  $c$ , and hence volume, with large errors. Using the determinative curves of Nolan (1969), the pyroxene is about  $\text{Hd}_{80}\text{Ac}_{20}$ . Aoki (1964) and Nolan (1969) have pointed out the limitations of the determinative curves when the pyroxene coexists with a melt. Consequently, this value is only approximate. Compositions determined by electron microprobe were inaccurate because of small crystal size and Na volatilization. Microprobe results indicate that  $(\text{Ca} + \text{Na}) < \text{Fe}$ , and obviously there must be some ferrosilite component in the pyroxene which moves the composition from the acmite-hedenbergite join.

The stability of amphibole on the ferrichterite bulk composition is greatly reduced at  $f_{\text{O}_2}$  above the WM buffer. Figure 3 shows the phase equilibria defined by the QFM buffer at variable  $P$  and  $T$ . A larger amount of  $\text{Fe}^{3+}$  is present here as indicated by the Mössbauer fit (D. Virgo, personal communication, 1972). Accordingly, 30–40 percent of the charge in the amphibole field was an acmitic pyroxene. Experiments at higher pressure (7 kbar) yielded somewhat greater amounts of  $\text{Fe}^{3+}$ -rich amphibole with a distinctly smaller unit-cell volume than amphibole on IW ( $929.7$  Å<sup>3</sup> vs  $936.0$  Å<sup>3</sup>). The amphibole may become more riebeckitic as larger amounts of  $\text{Fe}^{3+}$  appear and Ca, Na, and Fe are lost to the pyroxene. In order to prove the stability of the pyroxene in the amphibole field, amphibole prepared on IW was reacted on QFM and yielded amphibole + pyroxene. Between 1 and 7 kbar and  $535^\circ \pm 10^\circ\text{C}$ , amphibole + pyroxene decomposes to  $\text{Ac}_{67}\text{Hd}_{33}$  + fayalite + magnetite + quartz + vapor. At higher temperatures this assemblage undergoes partial melting:  $\text{Ac}_{67}\text{Hd}_{33}$  + quartz  $\rightleftharpoons$  hedenbergitic pyroxene + melt  $\pm$  fayalite  $\pm$  magnetite.  $\text{Ac}_{67}\text{Hd}_{33}$  was determined directly by microprobe analysis and from Nolan (1969) since no melt is present. Its unit-cell parameters as well as those of other pyroxenes grown in the bulk composition "ferrichterite" are given in Table 3. On the basis of estimates from Nolan (1969) with the reservations expressed previously, the pyroxene above the solidus is found to be somewhat more ferrous ( $\text{Hd}_{75}\text{Ac}_{25}$ ).

Problems with metastable formation of 1:2:6 Na-Fe silicate were encountered owing to the lesser buffering capacity of QFM. Starting materials containing  $\text{Fe}^0$ , buffered by QFM for a few days, invariably reacted to yield charges containing 1:2:6 Na-

TABLE 3. Unit Cell Parameters, Bulk Composition:  $\text{Na}_2\text{CaFe}_6\text{Si}_6\text{O}_{22}(\text{OH})_2$ 

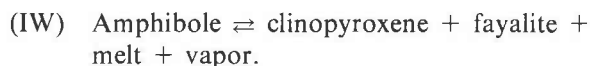
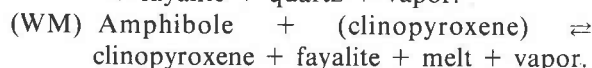
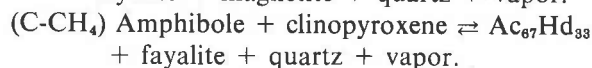
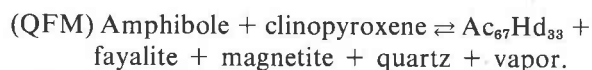
Phase	Coexisting phase(s)	$\bar{P}$ (bars)	$\bar{T}$ (°C)	$\bar{a}$ (Å)	$\bar{b}$ (Å)	$\bar{c}$ (Å)	$\bar{\beta}$	$\bar{V}$ (Å <sup>3</sup> )
Fe <sub>3</sub> O <sub>4</sub> -Fe <sub>2</sub> O <sub>3</sub> Buffer								
Cpx	H+Mt+Q	1000	700	9.696(5)*	8.844(5)	5.289(3)	106°47' (3)	434.2(0.3)
Fe <sub>2</sub> SiO <sub>4</sub> -SiO <sub>2</sub> -Fe <sub>3</sub> O <sub>4</sub> Buffer								
A	Cpx	7000	500	9.937(5)	18.180(9)	5.280(4)	103°27' (5)	927.7(0.7)
A	Cpx	4000	475	9.881(11)	18.136(8)	5.330(4)	103°46' (4)	927.7(0.9)
A	Cpx	4000	475	9.898(9)	18.146(9)	5.328(11)	103°57' (4)	929.0(0.9)
Cpx	Fa+Mt+Q	1000	700	9.698(10)	8.869(11)	5.282(5)	106°42' (7)	435.5(0.5)
Cpx	Fa+Mt+M	1000	820	9.744(4)	8.838(4)	5.471(18)	105°19' (6)	454.5(0.5)
Cpx	A	1000	475	9.746	8.855	5.280	106°28'	437.0
Fe-FeO Buffer								
Cpx	Fa+M	1000	800	9.809(4)	8.999(7)	5.288(18)	105°15' (7)	465.7(1.3)
A	...	10000	530	9.975(2)	18.226(6)	5.292(2)	103°37' (8)	935.0(0.5)
A	...	5000	530	9.990(3)	18.216(6)	5.303(2)	103°51' (2)	937.0(0.4)
A	...	2000	500	9.980(8)	18.227(6)	5.300(6)	103°44' (5)	936.5(0.6)

\*Parenthesized figures represent the estimated standard deviation (esd) in terms of least units cited for the value to their immediate left, thus 9.696(5) indicates an esd of 0.005.

Fe silicate if grown within the field of stable 1 : 2 : 6 Na-Fe silicate which occurs on IW. This region is approximately 600° to 750°C at pressures up to 4 kbar. Such charges, when resubmitted, converted to  $\text{Ac}_{67}\text{Hd}_{33}$  + fayalite + magnetite + quartz on QFM. Similar problems were found with amphibole. A ferrous amphibole may crystallize within a few days using a reduced mix, if it is held just beyond the stability limit of amphibole + clinopyroxene. In order to avoid these problems only materials equilibrated for several weeks on QFM were used for most reversal experiments.

Figure 4 displays the phase equilibria for the ferrichterite bulk composition at a  $P_{\text{total}}$  of 1 kbar with variable  $f_{\text{O}_2}$  and  $T$ . Within its field of stability the amphibole is on the ferrichterite bulk composition only at low  $f_{\text{O}_2}$  (IW). On buffers of progressively higher  $f_{\text{O}_2}$ , increasing amounts of pyroxene appear with amphibole and approach 30–40 percent of the charge on QFM buffer.

Maximum stability limits of amphibole in the ferrichterite bulk composition at  $P_{\text{total}} = 1$  kbar are: QFM,  $535^\circ \pm 10^\circ\text{C}$ ; C-CH<sub>4</sub>,  $580^\circ \pm 10^\circ\text{C}$ ; WM,  $760^\circ \pm 10^\circ\text{C}$ ; IW,  $715^\circ \pm 10^\circ\text{C}$ . Amphibole ± clinopyroxene decomposes according to the following reactions:



The subsolidus assemblage melts at high  $f_{\text{O}_2}$ :

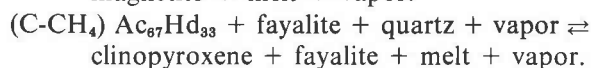
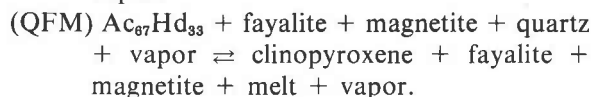
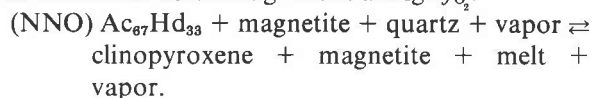


Table 3 gives the cell parameters of coexisting phases in the bulk composition ferrichterite. The decrease in cell volume at higher  $f_{\text{O}_2}$  suggests that the amphibole becomes a ferrichterite coexisting with an acmitic pyroxene. The pyroxene coexisting with melt greatly increases in  $a$ ,  $b$ , and  $V$  with a large decrease in  $\beta$  from QFM to IW. This result indicates an increase in acmite component as  $f_{\text{O}_2}$  is increased, if the data of Nolan (1969) are loosely applied. Judging from the gradual disappearance of 020 and 310 reflections as  $f_{\text{O}_2}$  decreases and from the limited unit-cell data, the conclusion is that the pyroxene reacts continuously with the melt and possibly the other solid phases as  $f_{\text{O}_2}$  is decreased. Na plus silica from the melt react with Fe to yield a more acmitic pyroxene at higher  $f_{\text{O}_2}$ . Such variations are not present in the subsolidus region. This may be a problem of slow reaction rates as pointed out by J. Holloway (personal communication, 1974). The pyroxene,  $\text{Ac}_{67}\text{Hd}_{33}$ , remains at constant composition on QFM and HM, as verified by the unit-cell dimen-

TABLE 4. Clinopyroxene Stability

$\bar{P}$ (kbar)	Buffer	$\bar{T}$ ( $\pm 10^\circ\text{C}$ )	
		Acmite (Bailey, 1969)	$\text{Ac}_{67}\text{Hd}_{33}$ (+Fa+Mt+Q)
1	HM	890	...
1	NNO	850	845
1	QFM	810	815

sions, the determinative curves of Nolan (1969), and the electron microprobe analyses. These observations show that a singular invariant point occurs just above the WM buffer at approximately  $770^\circ\text{C}$  at 1 kbar  $P_{\text{total}}$ . The dashed extension of the melting curve (Fig. 4) to higher  $f_{\text{O}_2}$  has been estimated using the data of Bailey (1969) for the melting of acmite, as shown in Table 4.

The partial melting of  $\text{Ac}_{67}\text{Hd}_{33}$  occurs under almost the same conditions as that of acmite. Another similarity is that  $\text{Ac}_{67}\text{Hd}_{33}$  (+ fayalite + magnetite + quartz + vapor) reacts to form amphibole (ferrichterite) at lower  $f_{\text{O}_2}$  and acmite also forms amphibole under similar conditions (riebeckite-arfvedsonite).

## Discussion

### Melting of a Hydrous Phase

The effect of an excess of  $\text{H}_2\text{O}$  upon the thermal decomposition of amphibole, if any, is less than  $10^\circ\text{C}$  for the  $P$ - $T$  range examined. Specifically, experiments at 1 kbar varied in excess  $\text{H}_2\text{O}$  from 0 to 12.9 wt percent, yet a  $10^\circ\text{C}$  reversal is observed. At 200 bars the excess  $\text{H}_2\text{O}$  varied from 1.9 to 27.1 wt percent, also with a  $10^\circ\text{C}$  reversal. To be more specific, at  $990^\circ\text{C}$  and 200 bars  $P_{\text{total}}$  the two experiments contained 1.9 and 22.9 wt percent excess  $\text{H}_2\text{O}$ . At  $1000^\circ\text{C}$  and 200 bars  $P_{\text{total}}$ , the two experiments contained 5.2 and 27.1 wt percent excess  $\text{H}_2\text{O}$ . Each set of bracketing

experiments resulted in the same phase assemblage, richterite at  $990^\circ\text{C}$  and  $\text{Fo} + \text{Di} + \text{En} + \text{M} + \text{V}$  at  $1000^\circ\text{C}$ . Not enough experiments were performed to prepare a detailed  $T$ - $X$  diagram for richterite- $\text{H}_2\text{O}$ . Consequently, the three possible melting relationships of richterite on the pseudobinary  $\text{Na}_2\text{O} \cdot \text{CaO} \cdot 5\text{MgO} \cdot 8\text{SiO}_2 - \text{H}_2\text{O}$  are presented schematically in Figure 5 (after Eggler, 1973). These are arranged in order of increasing total pressure. As the vapor-present fields sweep toward the left, it is possible to generate melts either more or less hydrous than amphibole. Some experiments in the amphibole field did have trace pyroxene, olivine, and glass. This result could be due to very slight inhomogeneity or nonstoichiometry of the mix. However, most experiments, regardless of  $\text{H}_2\text{O}$  content, were very nearly 100 percent amphibole. This observation along with those presented at the beginning of this paragraph suggests that Figure 5a is most valid for total pressure in the range 200 to 1000 bars.

As Figure 5 shows, in the presence of a melt the stability limit of amphibole may remain the same or decrease with addition of an excess of  $\text{H}_2\text{O}$ . An excellent example of the latter effect is observed in the work of Yoder and Kushiro (1969) in which  $\text{K}_2\text{O} \cdot 6\text{MgO} \cdot \text{Al}_2\text{O}_3 \cdot 6\text{SiO}_2 - \text{H}_2\text{O}$  is examined at a  $P_{\text{H}_2\text{O}}$  of 10 kbar. Their Figure 4 is topologically similar to Figure 5b here. If Figure 5a is valid for richterite, excesses of less than 27 percent  $\text{H}_2\text{O}$  do not significantly affect the maximum stability limit of amphibole.

### Crystal Chemistry

At 1 kbar the maximum stability limits of the richterites are: Fe-richterite (WM),  $760^\circ \pm 10^\circ\text{C}$ ; Mg-richterite,  $1030^\circ \pm 10^\circ\text{C}$  (see Table 5). Substitution of five ferrous irons for five magnesiums, causing a decreased linking of the silicon double chains, lowers the stability limit  $270^\circ\text{C}$  at 1 kbar. This lowering of the stability limit compares with  $210^\circ\text{C}$  under similar conditions for pargasite-ferropargasite (Boyd, 1959; Gilbert, 1966) and  $365^\circ\text{C}$  for tremolite-ferrotremolite (Boyd, 1959; Ernst, 1966).

The substitution  $2\text{Na} \rightleftharpoons \text{Ca}$  in tremolite, filling the vacant  $A$  site, greatly stabilizes the resulting richterite. The thermal stability limit is increased by  $200^\circ\text{C}$  at 1 kbar. Magnesioriebeckite (Ernst, 1960) on HM buffer is about  $100^\circ\text{C}$  less stable than richterite for the same reason. The substitution  $\text{CaAl}_3 \rightleftharpoons \text{NaMgSi}_2$ , transforming pargasite to richterite, results in only a slight decrease in stability of about  $15^\circ\text{C}$  at 1 kbar. The substitution of cations of similar

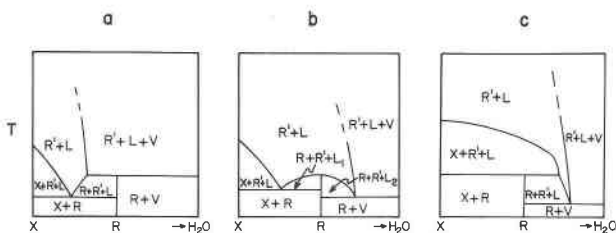


FIG. 5. Schematic isobaric  $T$ - $X$  equilibria for the compositional join  $x$ - $\text{H}_2\text{O}$ , where  $x = \text{Na}_2\text{O} \cdot \text{CaO} \cdot 5\text{MgO} \cdot 8\text{SiO}_2$ ,  $R$  = richterite,  $R'$  = incongruent melting products of richterite and  $x$ . Load pressure increases from right to left:  $P_a < P_b < P_c$ .

TABLE 5. Amphibole Stabilities at  $P_{\text{Tot}} = P_{\text{H}_2\text{O}}$  of 1000 Bars

Phase (buffer)	Site occupancy				Maximum thermal stability limit ( $T$ , °C)	Reference
	A	M <sub>4</sub>	M <sub>1</sub> +M <sub>2</sub> +M <sub>3</sub>	Si <sub>I</sub> +Si <sub>II</sub>		
Richterite	Na	Na, Ca	5Mg	8Si	1030	This paper
Ferrichterite (WM)	Na	Na, Ca	5Fe <sup>2+</sup>	8Si	760	This paper
Tremolite	□	2Ca	5Mg	8Si	830	Boyd, 1959
Ferrotremolite (IM)	□	2Ca	5Fe <sup>2+</sup>	8Si	465	Ernst, 1966
Magnesioriebeckite (HM)	□	2Na	3Mg, 2Fe <sup>3+</sup>	8Si	928	Ernst, 1960
Riebeckite (HM)	□	2Na	3Fe <sup>2+</sup> , 2Fe <sup>3+</sup>	8Si	496	Ernst, 1962
Pargasite	Na	2Ca	4Mg, Al	6Si, 2Al	1045	Boyd, 1959
Ferropargasite (WM)	Na	2Ca	4Fe <sup>2+</sup> , Al	6Si, 2Al	835	Gilbert, 1966

size, while keeping the A site filled, has little effect on thermal stability.

The iron-bearing end members have been discussed at some length in a previous paper (Charles, 1974). Briefly, local charge imbalance due to Na in the M(4) site greatly decreases amphibole stability at higher  $f_{\text{O}_2}$  (QFM and NNO) when compared with ferropargasite (Gilbert, 1966), which has complete local charge balance. On the IW buffer, where the ferrichterite contains 95 percent ferrous iron, the thermal stability limit is still somewhat less than that of ferropargasite (80°C at 1 kbar) owing to the decreased linking of the double chains of silicon tetrahedra in ferrichterite. Amphibole chains are linked primarily by the M(2) and M(4) cations. In richterite the mean size of the cations in M(2) is much greater than in ferropargasite (2Fe<sup>2+</sup> vs Al + Fe<sup>2+</sup>) with M(4) holding cations of similar size. The effect is also seen in the smaller *b* dimension of pargasite (18.14 Å vs 18.22 Å). Once again ferrotremolite and riebeckite are much less stable than ferrichterite owing to the vacancy in A.

Currently under investigation is the series pargasite-ferropargasite, which does not involve problems of local charge balance. Combining these data with a study of tremolite-ferrotremolite would yield valuable information for the interpretation of most natural hornblendes.

### Acknowledgments

The author would like to thank Drs. David R. Wones, Hatten S. Yoder, Jr., Friedrich Seifert, Thomas Brown, and F. R. Boyd for their many useful comments and suggestions aiding in this study. Special thanks go to Dr. Hatten S. Yoder, Jr., for the use of his equipment and support at the Geophysical Laboratory, Carnegie Institution of Washington. I also wish to thank Miss Dolores M. Thomas for careful editing of the manuscript.

This study was supported by National Science Foundation grants GA1109 and GA13092 to Dr. David R. Wones and by the Geophysical Laboratory.

### References

- AOKI, K. (1964) Clinopyroxenes from alkaline rocks of Japan. *Am. Mineral.* **49**, 1199-1223.
- BAILEY, D. K. (1969) The stability of acmite in the presence of H<sub>2</sub>O. *Am. J. Sci.* **267A**, 1-16.
- BOYD, F. R. (1959) Hydrothermal investigations of the amphiboles. In P. H. Abelson, Ed., *Researches in Geochemistry*, John Wiley and Sons, Inc., New York, p. 377-396.
- BOYD, F. R., AND J. F. SCHAIRER (1964) The system MgSiO<sub>3</sub>-CaMgSi<sub>2</sub>O<sub>6</sub>. *J. Petrol.* **5**, 275-309.
- CHARLES, R. W. (1974) The physical properties of the hydrous Mg-Fe richterites. *Am. Mineral.* **59**, 518-528.
- EGGLER, D. H. (1973) Principles of melting of hydrous phases in silicate melt. *Carnegie Inst. Wash. Year Book*, **72**, 491-495.
- ERNST, W. G. (1960) Stability relations of magnesioriebeckite. *Geochim. Cosmochim. Acta*, **19**, 10-40.
- (1962) Synthesis, stability relations, and occurrence of riebeckite and riebeckite-arfvedsonite solid solutions. *J. Geol.* **70**, 689-736.
- (1966) Synthesis and stability relations of ferrotremolite. *Am. J. Sci.* **264**, 37-65.
- (1968) *Amphiboles*. Springer Verlag, New York.
- EUGSTER, H. P. (1957) Heterogeneous reactions involving oxidation and reduction at high pressures and temperatures. *J. Chem. Phys.* **26**, 1760-1761.
- , AND G. B. SKIPPEN (1967) Igneous and metamorphic reactions involving gas equilibria. In P. H. Abelson, Ed., *Researches in Geochemistry*, Vol. 2, John Wiley and Sons, Inc., New York, p. 377-396.
- , AND D. R. WONES (1962) Stability relations of the ferruginous biotite annite. *J. Petrol.*, **3**, 82-125.
- EVANS, H. T., JR., D. E. APPLEMAN, AND D. S. HANDWERKER (1963) The least-squares refinement of crystal unit cells with powder diffraction data by an automatic computer indexing method (abstr.). *Am. Crystallogr. Assoc. Annu. Meet., Cambridge, Mass., Program*, p. 42-43.
- FISHER, G. W., AND L. G. MEDARIS (1969) Cell dimensions and X-ray determinative curve for synthetic Mg-Fe olivines. *Am. Mineral.* **54**, 741-753.
- FORBES, W. C. (1971) Synthesis and stability relations on richterite. *Am. Mineral.* **56**, 997-1004.
- GILBERT, M. C. (1966) Synthesis and stability relations of the hornblende ferropargasite. *Am. J. Sci.* **264**, 698-742.
- NOLAN, J. (1969) Physical properties of synthetic and natural pyroxenes in the system diopside-hedenbergite-acmite. *Mineral. Mag.* **37**, 216-229.

- OLSEN, E. (1967) A new occurrence of roedderite and its bearing on osumilite-type minerals. *Am. Mineral.* **52**, 1519-1523.
- SAHAMA, TH. G., AND K. HYTÖNEN (1958) Calcium bearing magnesium iron olivines. *Am. Mineral.* **43**, 862-871.
- SCHAIRER, J. F., AND H. S. YODER, JR. (1970) The join  $\text{Na}_2\text{O} \cdot 5\text{MgO} \cdot 12\text{SiO}_2$ -sodium disilicate and  $2\text{Na}_2\text{O} \cdot 3\text{MgO} \cdot 5\text{SiO}_2$ -sodium disilicate in the system  $\text{Na}_2\text{O}-\text{MgO}-\text{SiO}_2$ . *Carnegie Inst. Wash. Year Book*, **69**, 157-159.
- SHAW, H. R. (1967) Hydrogen osmosis in hydrothermal experiments. In, P. H. Abelson, Ed., *Researches in Geochemistry*, Vol. 2, John Wiley and Sons, Inc., New York, p. 521-541.
- TUTTLE, O. F. (1949) Two pressure vessels for silicate-water studies. *Bull. Geol. Soc. Amer.*, **60**, 1727-1729.
- YODER, H. S., JR., AND I. KUSHIRO (1969) Melting of a hydrous phase: phlogopite. *Am. J. Sci.* **267A**, 558-582.

*Manuscript received, February 25, 1974; accepted for publication, December 30, 1974.*